Channel Shaping Using Reconfigurable Intelligent Surfaces: From Diagonal to Beyond

Yang Zhao, *Member, IEEE,* Hongyu Li, *Graduate Student Member, IEEE,*
Yijie Mao, *Member, IEEE,* Shanpu Shen, *Member, IEEE,* and Bruno Clerckx, *Fellow, IEEE*

I. Assumption

We introduce Beyond-Diagonal (BD) Reconfigurable Intelligent Surface (RIS) in Multiple-Input Multiple-Output (MIMO) Point-to-point Channel (PC) and Interference Channel (IC). All proposals are based on assumption of *asymmetric* passive BD RIS, i.e., symmetry constraint $\mathbf{\Theta}_g = \mathbf{\Theta}_g^{\mathsf{T}}$ is relaxed. This is feasible when asymmetric passive components (e.g., ring hybrids and branch-line hybrids) [1] are available. This assumption was also made in Hongyu's papers [2], [3]. For quadratic problems, the proposed algorithms may be extended to symmetric BD RIS by replacing singular value decomposition with Takagi factorization [4].

II. MIMO-PC

A. Channel Power Maximization

Consider a BD RIS with N^{S} elements, which is divided into G groups of equal L elements.

$$\max_{\mathbf{\Theta}} \quad \left\|\mathbf{H}^{\mathrm{D}}+\sum\nolimits_g \mathbf{H}_g^{\mathrm{B}}\mathbf{\Theta}_g\mathbf{H}_g^{\mathrm{F}}\right\|_{\mathrm{F}}^2 \tag{1a}$$

$$\text{s.t.} \quad \mathbf{\Theta}_g^{\mathsf{H}}\mathbf{\Theta}_g=\mathbf{I}, \quad \forall g\in\mathcal{G}\triangleq\{1,...,G\}. \tag{1b}$$

For *symmetric* BD-RIS, the problem has been solved in

- Matteo's paper [5]: SISO and equivalent[1];
- Ignacio's paper [6]: SISO and directless MISO/SIMO.

Remark 1. *The difficulty of* (1) *is that the RIS needs to balance the additive (direct-indirect) and multiplicative (forward-backward) eigenspace alignment. Interestingly, it has the same form as the* weighted orthogonal Procrustes problem *[7]:*

$$\min_{\mathbf{\Theta}} \quad \|\mathbf{C}-\mathbf{A}\mathbf{\Theta}\mathbf{B}\|_{\mathrm{F}}^2 \tag{2a}$$

$$\text{s.t.} \quad \mathbf{\Theta}^{\mathsf{H}}\mathbf{\Theta}=\mathbf{I}. \tag{2b}$$

There exists no trivial solution to (2)*. One lossy transformation, by moving* $\mathbf{\Theta}$ *to one side [8], formulates a standard orthogonal Procrustes problem:*

$$\min_{\mathbf{\Theta}} \quad \|\mathbf{A}^{\dagger}\mathbf{C}-\mathbf{\Theta}\mathbf{B}\|_{\mathrm{F}}^2 \tag{3a}$$

$$\text{s.t.} \quad \mathbf{\Theta}^{\mathsf{H}}\mathbf{\Theta}=\mathbf{I}. \tag{3b}$$

(3) *has a global optimal solution* $\mathbf{\Theta}^{\star}=\mathbf{U}\mathbf{V}^{\mathsf{H}}$*, where* $\mathbf{U}$ *and* $\mathbf{V}$ *are left and right singular matrix of* $\mathbf{A}^{\dagger}\mathbf{C}\mathbf{B}^{\mathsf{H}}$ *[9]. This low-complexity solution will be compared with the one proposed later.*

[1]Single-stream MIMO with given precoder and combiner.

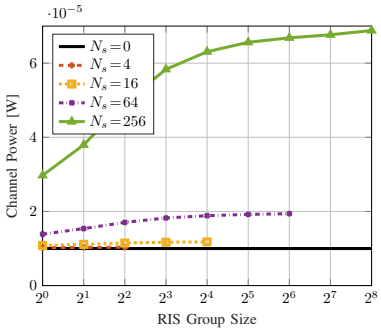

Fig. 1. Average channel power versus RIS elements N^{S} and group size L for $(N^{\mathrm{T}},N^{\mathrm{R}})=(8,4)$, $(\Lambda^{\mathrm{D}},\Lambda^{\mathrm{F}},\Lambda^{\mathrm{B}})=(65,54,46)$dB.

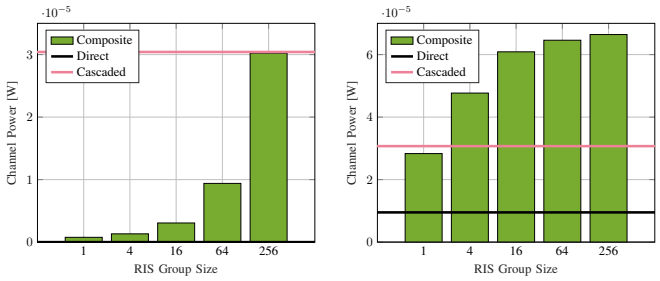

(a) Without Direct Link (b) With Direct Link

Fig. 2. Average channel power versus RIS group size L for $(N^{\mathrm{T}},N^{\mathrm{S}},N^{\mathrm{R}})=(8,256,4)$, $(\Lambda^{\mathrm{D}},\Lambda^{\mathrm{F}},\Lambda^{\mathrm{B}})=(65,54,46)$dB.

Inspired by [10], we propose an iterative algorithm to solve (1). The idea is to successively approximate the quadratic objective with a sequence of affine functions and solve the resulting subproblems in closed form.

Proposition 1. *Start from any* $\mathbf{\Theta}^{(0)}$*, the sequence*

$$\mathbf{\Theta}_g^{(r+1)}=\mathbf{U}_g^{(r)}\mathbf{V}_g^{(r)}, \quad \forall g \tag{4}$$

converges to a stationary point of (1)*, where* $\mathbf{U}_g^{(r)}$ *and* $\mathbf{V}_g^{(r)}$ *are left and right singular matrix of*

$$\begin{aligned}\mathbf{M}_g^{(r)}=&\mathbf{H}_g^{\mathrm{B}\,\mathsf{H}}\mathbf{H}^{\mathrm{D}}\mathbf{H}_g^{\mathrm{F}\,\mathsf{H}}+\sum_{g'<g}\mathbf{H}_{g'}^{\mathrm{B}\,\mathsf{H}}\mathbf{H}_{g'}^{\mathrm{B}}\mathbf{\Theta}_{g'}^{(r+1)}\mathbf{H}_{g'}^{\mathrm{F}}\mathbf{H}_{g'}^{\mathrm{F}\,\mathsf{H}}\\&+\sum_{g'\geq g}\mathbf{H}_{g'}^{\mathrm{B}\,\mathsf{H}}\mathbf{H}_{g'}^{\mathrm{B}}\mathbf{\Theta}_{g'}^{(r)}\mathbf{H}_{g'}^{\mathrm{F}}\mathbf{H}_{g'}^{\mathrm{F}\,\mathsf{H}}.\end{aligned} \tag{5}$$

Proof. To be added. □

Fig. 1 shows that, apart from adding reflecting elements N^{S}, increasing the group size L also improves the channel

power. This behavior is more pronounced for a large RIS. For example, the gain of pairwise connection is 2.8 % for $N^{\mathrm{S}}=16$ and 28 % for $N^{\mathrm{S}}=256$. It implies that the channel shaping capability of BD RIS scales with group size L.

Fig. 2b and 2a compare the average channel power without and with direct link. "Cascaded" means the *power product* of the forward and backward channels. We observe that diagonal RIS wastes substantial cascaded power and struggles to align the direct-indirect eigenspace. When the direct link is absent, only 2.6 % of available power is utilized by diagonal RIS while 100 % power is recycled by fully-connected RIS. When the direct link is present, the proposed BD RIS design can balance the direct-indirect and forward-backward eigenspace alignment for an optimal channel boost. It is worth noting that, when L is sufficiently large, the composite channel power surpasses the power sum of direct and cascaded channels, thanks to the constructive *amplitude superposition* of direct and cascaded channels. This again emphasizes the advantage of in-group connection of BD RIS.

B. Rate Maximization

The problem is formulated w.r.t. precoder (instead of transmit covariance matrix) for reference:

$$\max_{\mathbf{W},\boldsymbol{\Theta}} \quad \operatorname{logdet}\left(\mathbf{I}+\frac{\mathbf{W}^{\mathsf{H}}\mathbf{H}^{\mathsf{H}}\mathbf{H}\mathbf{W}}{\sigma_n^2}\right) \tag{6a}$$

$$\text{s.t.} \quad \|\mathbf{W}\|_{\mathrm{F}}^2 \le P, \tag{6b}$$

$$\boldsymbol{\Theta}_g^{\mathsf{H}}\boldsymbol{\Theta}_g=\mathbf{I}, \quad \forall g. \tag{6c}$$

(6) is jointly non-convex and solved by Alternating Optimization (AO). For a given $\boldsymbol{\Theta}$, the optimal precoder is given by

$$\mathbf{W}^{\star}=\mathbf{V}\mathbf{S}^{\star 1/2}, \tag{7}$$

where $\mathbf{V}$ is right singular matrix of $\mathbf{H}$ and $\mathbf{S}^{\star}$ is a diagonal matrix of the water-filling power allocation. For a given $\mathbf{W}$, we update $\boldsymbol{\Theta}$ by Riemannian Conjugate Gradient (RCG) method along the geodesics [11].

Remark 2. *A geodesic refers to the shortest path between two points in a Riemannian manifold. Unitary constraint* (6c) *translates to a Stiefel manifold where the geodesics have simple expressions described by the exponential map [12].*

For general optimization problems with block unitary constraint, the adapted RCG method at iteration r for block g is summarized below, where $f\left(\boldsymbol{\Theta}_g^{(r)}\right)$ is the objective function also evaluated over $\left\{\{\boldsymbol{\Theta}_{g'}^{(r+1)}\}_{g'<g},\{\boldsymbol{\Theta}_{g'}^{(r)}\}_{g'>g}\right\}$.

1) Compute the Euclidean gradient

$$\nabla_g^{\mathrm{E}(r)}=\frac{\partial f\left(\boldsymbol{\Theta}_g^{(r)}\right)}{\partial \boldsymbol{\Theta}_g^{*}}; \tag{8}$$

2) Translate to the Riemannian gradient

$$\nabla_g^{\mathrm{R}(r)}=\nabla_g^{\mathrm{E}(r)}\boldsymbol{\Theta}_g^{(r)\mathsf{H}}-\boldsymbol{\Theta}_g^{(r)}\nabla_g^{\mathrm{E}(r)\mathsf{H}}; \tag{9}$$

3) Determine the weight factor

$$\gamma_g^{(r)}=\frac{\operatorname{tr}\left(\left(\nabla_g^{\mathrm{R}(r)}-\nabla_g^{\mathrm{R}(r-1)}\right)\nabla_g^{\mathrm{R}(r)\mathsf{H}}\right)}{\operatorname{tr}\left(\nabla_g^{\mathrm{R}(r-1)}\nabla_g^{\mathrm{R}(r-1)\mathsf{H}}\right)}; \tag{10}$$

Algorithm 1: RCG Method for RIS MIMO-PC Rate Maximization

Input: $\mathbf{H}^{\mathrm{D}}$, $\mathbf{H}^{\mathrm{F}}$, $\mathbf{H}^{\mathrm{B}}$, $\mathbf{W}$, L, σ_n^2
Output: $\boldsymbol{\Theta}^{\star}$
1: $r\leftarrow 0$, $\boldsymbol{\Theta}^{(0)}$
2: **Repeat**
3: $\quad r\leftarrow r+1$
4: $\quad$ **For** $g\leftarrow 1$ to G
5: $\quad\quad \boldsymbol{\Theta}_g^{(r)}\leftarrow$ (14), (9)–(13)
6: $\quad$ **End For**
7: **Until** $|R^{(r)}-R^{(r-1)}|/R^{(r-1)}\le\epsilon$

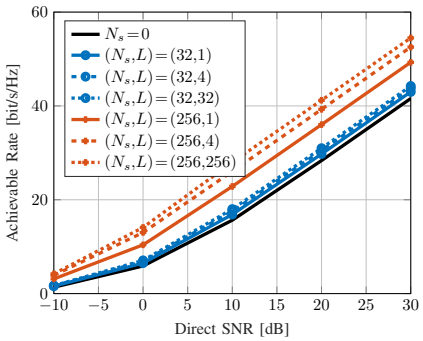

Fig. 3. Average achievable rate versus RIS elements N^{S} and group size L for $(N^{\mathrm{T}},N^{\mathrm{R}})=(8,4)$, $(\Lambda^{\mathrm{D}},\Lambda^{\mathrm{F}},\Lambda^{\mathrm{B}})=(65,54,46)$dB.

4) Compute the conjugate direction

$$\mathbf{D}_g^{(r)}=\nabla_g^{\mathrm{R}(r)}+\gamma_g^{(r)}\mathbf{D}_g^{(r-1)}; \tag{11}$$

5) Determine the Armijo step size[2]

$$\mu_g^{(r)}=\underset{\mu_g}{\operatorname{argmax}} f\left(\exp\left(\mu_g\mathbf{D}_g^{(r)}\right)\boldsymbol{\Theta}_g^{(r)}\right); \tag{12}$$

6) Perform rotational update along local geodesics

$$\boldsymbol{\Theta}_g^{(r+1)}=\exp\left(\mu_g^{(r)}\mathbf{D}_g^{(r)}\right)\boldsymbol{\Theta}_g^{(r)}. \tag{13}$$

Remark 3. *The adapted RCG method leverages the fact that block unitary matrices are closed under multiplication (but not necessarily under addition). Its advantage over universal manifold optimization [13], [14] is trifold:*

- *No retraction is involved;*
- *Lower computational complexity per iteration [12];*
- *Faster convergence thanks appropriate operational space.*

The complex derivative of (6a) w.r.t. RIS block g is

$$\frac{\partial R}{\partial \boldsymbol{\Theta}_g^{*}}=\frac{1}{\sigma_n^2}\mathbf{H}_g^{\mathrm{B}\mathsf{H}}\mathbf{H}\mathbf{W}\left(\mathbf{I}+\frac{\mathbf{W}^{\mathsf{H}}\mathbf{H}^{\mathsf{H}}\mathbf{H}\mathbf{W}}{\sigma_n^2}\right)^{-1}\mathbf{W}^{\mathsf{H}}\mathbf{H}_g^{\mathrm{F}\mathsf{H}}. \tag{14}$$

Algorithm 1 summarizes the adapted RCG method for the RIS rate maximization subproblem.

Fig. 3 illustrates how RIS configuration influences the MIMO PC achievable rate. To ensure a 20 bit/s/Hz transmission, an Signal-to-Noise Ratio (SNR) of 13.5 dB is required for a 8T4R system. This value decreases to 12.5 dB (resp. 8 dB) when 32- (resp. 256-) element diagonal RIS is present. If tetrads can be formed in BD RIS, the SNR can be reduced by another 20 %

[2]To double the step size, simply square the argument instead of recomputing the matrix exponential, i.e., $\exp(2\mu_g\mathbf{D}_g)=\exp^2(\mu_g\mathbf{D}_g)$.

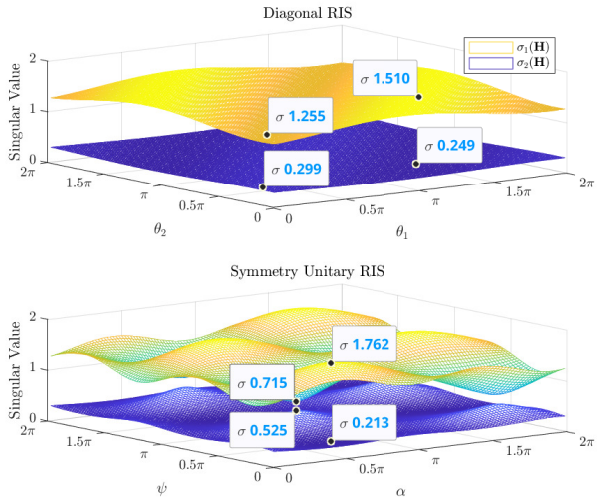

Fig. 4. Channel singular value shaping by diagonal and symmetry unitary RIS for $(N^{\mathrm{T}},N^{\mathrm{S}},N^{\mathrm{R}})=(2,2,2)$ without direct link.

(resp. $44\,\%$). Further increase in L yields a marginal gain and incurs $\mathcal{O}(L^2)$ connections. We thus conclude dyadic or tetradic BD RIS usually strike a good balance between performance and complexity.

C. Channel Singular Value Redistribution

In this subsection, we first show the channel shaping advantage of BD RIS by a toy example, then analyzes this *capability* under specific setups. Finally, we characterize the *Pareto front* of channel singular values via optimization approach.

Consider a toy example with $(N^{\mathrm{T}},N^{\mathrm{S}},N^{\mathrm{R}})=(2,2,2)$ and assume the direct link is absent. The diagonal RIS is $\mathbf{\Theta}^{\mathrm{D}}=\mathrm{diag}(e^{\jmath\theta_1},e^{\jmath\theta_2})$ while the unitary RIS has 4 independent angular parameters

$$\mathbf{\Theta}^{\mathrm{U}}=e^{\jmath\phi}\begin{bmatrix} e^{\jmath\alpha}\cos\psi & e^{\jmath\beta}\sin\psi \\ -e^{-\jmath\beta}\sin\psi & e^{-\jmath\alpha}\cos\psi \end{bmatrix}. \tag{15}$$

When the direct link is absent, ϕ has no impact on the singular value because $\mathrm{sv}(e^{\jmath\phi}\mathbf{A})=\mathrm{sv}(\mathbf{A})$. For a fair comparison, we enforce *symmetry* with $\beta=\pi/2$. Fig. 4 illustrates all possible channel singular values achieved by diagonal and symmetry unitary RIS. Clearly, BD RIS provides a much wider dynamic range of $\sigma_1(\mathbf{H})$ and $\sigma_2(\mathbf{H})$ than diagonal RIS, despite using the same number of elements and parameters. A larger gap is expected when the symmetry constraint can be relaxed.

1) Rank-1 Indirect Channel: When the RIS is in the vicinity of the transmitter / receiver, the forward / backward channel is often rank-1. The indirect channel is also rank-1 because

$$\mathrm{rank}(\mathbf{H}^{\mathrm{B}}\mathbf{\Theta}\mathbf{H}^{\mathrm{F}})\le\min\big(\mathrm{rank}(\mathbf{H}^{\mathrm{B}}),\mathrm{rank}(\mathbf{\Theta}),\mathrm{rank}(\mathbf{H}^{\mathrm{F}})\big). \tag{16}$$

REFERENCES

[1] H.-R. Ahn, *Asymmetric Passive Components in Microwave Integrated Circuits*. Wiley, 2006. [Online]. Available: https://books.google.co.uk/books?id=X6WdLbOuSNQC

[2] H. Li, S. Shen, and B. Clerckx, "Beyond diagonal reconfigurable intelligent surfaces: From transmitting and reflecting modes to single-, group-, and fully-connected architectures," *IEEE Transactions on Wireless Communications*, vol. 22, pp. 2311–2324, 4 2023.

[3] ——, "Beyond diagonal reconfigurable intelligent surfaces: A multi-sector mode enabling highly directional full-space wireless coverage," *IEEE Journal on Selected Areas in Communications*, vol. 41, pp. 2446–2460, 8 2023.

[4] R. A. Horn and C. R. Johnson, *Matrix Analysis*. Cambridge University Press, 2012. [Online]. Available: https://books.google.co.uk/books?id=O7sgAwAAQBAJ

[5] M. Nerini, S. Shen, and B. Clerckx, "Closed-form global optimization of beyond diagonal reconfigurable intelligent surfaces," *IEEE Transactions on Wireless Communications*, pp. 1–1, 2023. [Online]. Available: https://ieeexplore.ieee.org/document/10155675/

[6] I. Santamaria, M. Soleymani, E. Jorswieck, and J. Gutiérrez, "Snr maximization in beyond diagonal ris-assisted single and multiple antenna links," *IEEE Signal Processing Letters*, vol. 30, pp. 923–926, 2023. [Online]. Available: https://ieeexplore.ieee.org/document/10187688/

[7] J. C. Gower and G. B. Dijksterhuis, *Procrustes Problems*. OUP Oxford, 2004. [Online]. Available: https://books.google.co.uk/books?id=kRRREAAAQBAJ

[8] T. Bell, "Global positioning system-based attitude determination and the orthogonal procrustes problem," *Journal of Guidance, Control, and Dynamics*, vol. 26, pp. 820–822, 9 2003. [Online]. Available: https://arc.aiaa.org/doi/10.2514/2.5117

[9] G. H. Golub and C. F. V. Loan, *Matrix Computations*. Johns Hopkins University Press, 2013. [Online]. Available: https://jhupbooks.press.jhu.edu/title/matrix-computations

[10] F. Nie, R. Zhang, and X. Li, "A generalized power iteration method for solving quadratic problem on the stiefel manifold," *Science China Information Sciences*, vol. 60, p. 112101, 11 2017. [Online]. Available: http://link.springer.com/10.1007/s11432-016-9021-9

[11] T. Abrudan, J. Eriksson, and V. Koivunen, "Conjugate gradient algorithm for optimization under unitary matrix constraint," *Signal Processing*, vol. 89, pp. 1704–1714, 9 2009. [Online]. Available: https://linkinghub.elsevier.com/retrieve/pii/S0165168409000814

[12] T. E. Abrudan, J. Eriksson, and V. Koivunen, "Steepest descent algorithms for optimization under unitary matrix constraint," *IEEE Transactions on Signal Processing*, vol. 56, pp. 1134–1147, 3 2008. [Online]. Available: http://ieeexplore.ieee.org/document/4436033/

[13] P.-A. Absil, R. Mahony, and R. Sepulchre, *Optimization Algorithms on Matrix Manifolds*. Princeton University Press, 2009. [Online]. Available: https://books.google.co.uk/books?id=NSQGQeLN3NcC

[14] C. Pan, G. Zhou, K. Zhi, S. Hong, T. Wu, Y. Pan, H. Ren, M. D. Renzo, A. L. Swindlehurst, R. Zhang, and A. Y. Zhang, "An overview of signal processing techniques for ris/irs-aided wireless systems," *IEEE Journal of Selected Topics in Signal Processing*, vol. 16, pp. 883–917, 8 2022. [Online]. Available: https://ieeexplore.ieee.org/document/9847080/